H13A-1173 Uncertainty and Characterization of the Baton Rouge Fault System in a Bayesian Framework

H13A Characterization of Fault Zone Hydrology III | AGU Fall Meeting 2011, San Francisco, USA | 5-9 December

Ahmed S. Elshall[1], Frank T.-C. Tsai[1], Jeffrey S. Hanor[2]
[1]Department of Civil and Environmental Engineering, Louisiana State University , [2]Department of Geology and Geophysics, Louisiana State University
E-mail: aelsha1@lsu.edu; ftsai@lsu.edu; hanor@lsu.edu

[1] Introduction

Hydrostratigraphy modelers are faced with competing propositions about different components of the conceptual model (e.g. model data sets, calibration data sets, mathematical models, geological structure assumptions, modeling decisions, parameterization schemes, etc.)

- How to be certain about selecting the correct proposition for each model component out of numerous competing propositions?
- How to bridge the gap between synthetic mental principles (e.g. mathematical expressions and modeling decisions) and empirical observations (e.g. model data and calibration data) when uncertainty exists on both sides?

Under the stance of objective Bayesianism, we extend the BMA work of Tsai and Li [2008] and Li and Tsai [2009] to maximum likelihood hierarchical Bayesian model averaging (ML-HBMA) as an epistemic framework to represent our current state of knowledge to segregate different sources of uncertainty, and evaluate competing propositions for each source of uncertainty.

[2] Case Study

We apply this method to characterize the uncertainty of the Baton Rouge fault system in Louisiana consisting of

1) Baton Rouge (BR) fault, which is of particular importance from a resource standpoint since it acts as a conduit-barrier to a series of fresh water and brackish aquifers north and south of the fault, respectively
2) Denham Springs-Scotlandville (DSS) fault, in which we investigate the fault throw for the first time in this area, since previous studies [e.g. Rollo,1969] assume no fault throw

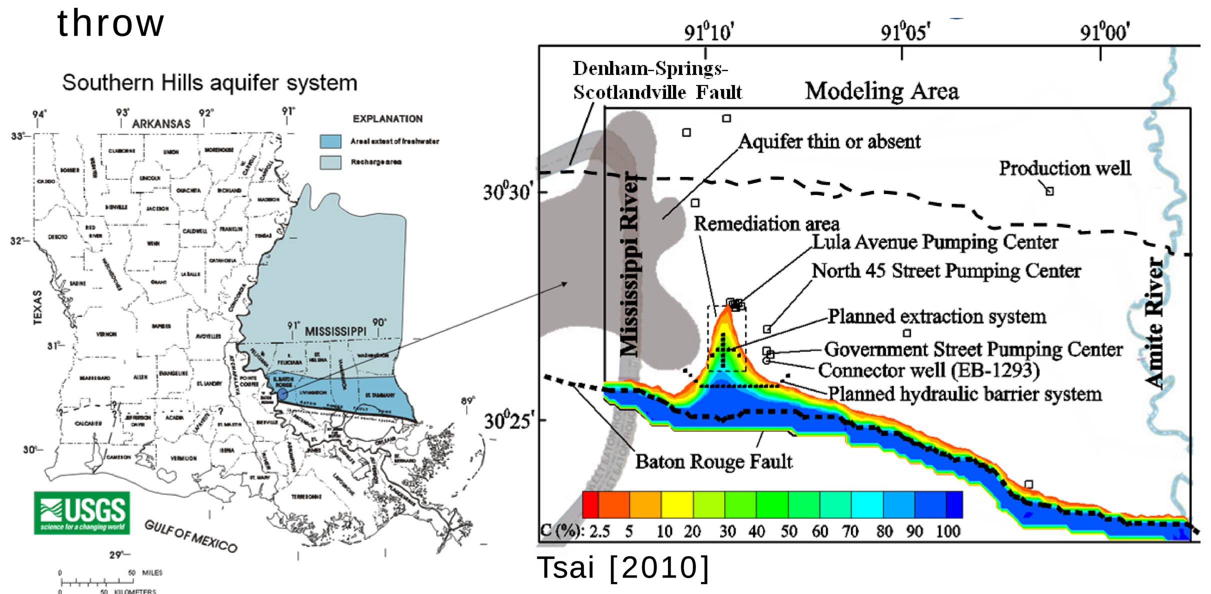

Figure (1) By considering only the BR fault similar to previous studies, we divide our modeling domain into two subdomains. By considering the BR and DSS faults, the model has three subdomains.

When characterizing complex spatial variations of subsurface geology, uncertainty exists resulting in multiple plausible hydrostratigraphy fault models. We consider four hierarchies of uncertainty as follows:

1) Calibration data sets [2 data sets]
2) Geological stationarity assumptions of different aquifer subdomains [2 assumptions]
3) Geological structures with respect to the fault system [2 conceptualizations]
4) Mathematical structures [3 mathematical models]

Each hierarchy represents one level of uncertainty with its different competing propositions, resulting in 24 different competing conceptual models.

References

- Hansen, N. (2006). The CMA Evolution Strategy: A Comparing Review. In J.A. Lozano, P. Larrañga, I. Inza and E. Bengoetxea (eds.). Towards a new evolutionary computation. Advances in estimation of distribution algorithms. pp. 75-102, Springer
- Rollo,J.R. (1969), Saltwater encroachment in aquifer of the Baton Rouge Area, Louisiana, State of Louisiana. Office of Public works, Water Resources Bulletin No., 13, p.45.
- Li X. , and F.T.-C. Tsai (2009), Bayesian model averaging for groundwater head prediction and uncertainty analysis using multimodel and multimethod. Water Resources Research 45,W09403, doi:10.1029/2008WR007488
- Tsai, F. T.-C. (2010), Bayesian model averaging assessment on ground water management under model structure uncertainty, Stochastic Environmental Research and Risk Assessment, doi:10.1007/s00477-010-0382-3.
- Tsai, F. T.-C., and X. Li (2008), Groundwater inverse modeling for hydraulic conductivity estimation using Bayesian model averaging and variance window, Water Resources Research, 44, W09434, doi:10.1029/2007WR006576

Acknowledgements: The project is partially funded by the National Science Foundation EAR-10450646, the USGS-NIWR under Grant No. G10AP00136, and the Louisiana Water Resources Research Institute.

[3] Hydrostratigraphy Method

We utilize geophysical logs and local geological information, to construct indicator-kriging hydrostratigraphic fault model

$$I(\mathbf{x},v)=\begin{cases}1 & v\in \text{Sand}, \quad v(\mathbf{x})>\text{Shale Baseline}\\ 0 & v\in \text{Clay}, \quad v(\mathbf{x})<\text{Shale Baseline}\end{cases}$$

We use 288 geophysical logs. Automatic interpretation of electrical resistivity (ER) curves is inaccurate (Figure 2). Manual interpretation using ER, spontaneous-potential (SP) and gamma ray (GR) curves reduces data interpretation uncertainty (Figure 3)

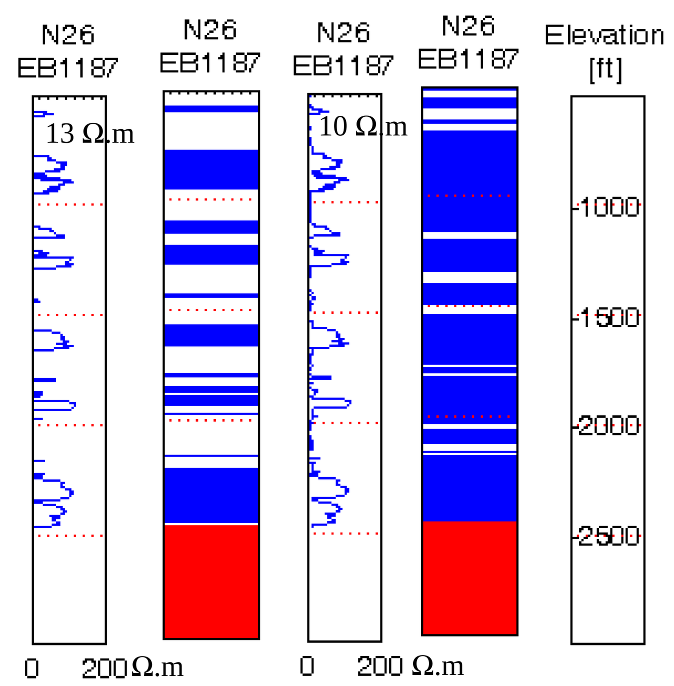

Figure(2) decreasing bed boundary shale baseline from 13Ω.m to 10Ω.m leads to more sand units(blue color)

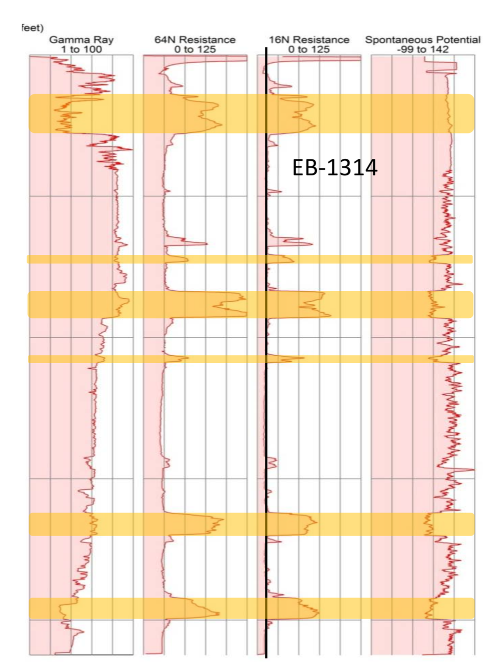

Figure(3) Manual delineation of sand sequences using ER, SP and GR curves

Vertical discretization is every 0.305m (1 foot) , with measurement points varying from 800 to 3200 for each borehole depending on the borehole depth.

[4] Calibration Method

We calibrate the hydrostratigraphic model with the driller logs, using the covariance matrix adaptation-evolution strategy (CMA-ES) [Hansen, 2006], which is a state-of-the-science stochastic local search method.

The decision variables of the inverse problem are:

1) Dipping angle Φ, which affects the variogram structure through establishing correlations between horizontal measurement points. We set $0 < \Phi < 1.0$ %
2) Sand-clay probability cutoff ω, for rounding estimated values of indicator kriging. We set $0.3 < \omega < 0.7$

Given the sand ratio 38.78%, to avoid calibration bias toward clay over sand, the objective function separates the error to two least square error terms for sand and clay with w=0.5

$$f = wR_{sand} + (1-w)R_{clay}$$

[5] Uncertainty Method

After calibrating the 24 models, we apply ML-HBMA method to calculate the ensemble weighted model average, within-model covariance and between-model covariance.

$$\Pr\left(\mathbf{D}|\mathrm{M}\{\mathrm{n}\}^{(\mathrm{p})},\mathrm{M}\{\mathrm{n}+1\}_{\mathrm{q}}^{(\mathrm{p})}\right)\approx \exp\left[-\frac{1}{2}\mathrm{BIC}_{\mathrm{q}}^{(\mathrm{p})}\right]$$

$$BIC_q^{(p)} = -2\ln Pr\left(\boldsymbol{D}|M\{n\}^{(p)},M\{n+1\}_q^{(p)},\beta_q^{(p)}\right)+w_q^{(p)}\ln m$$

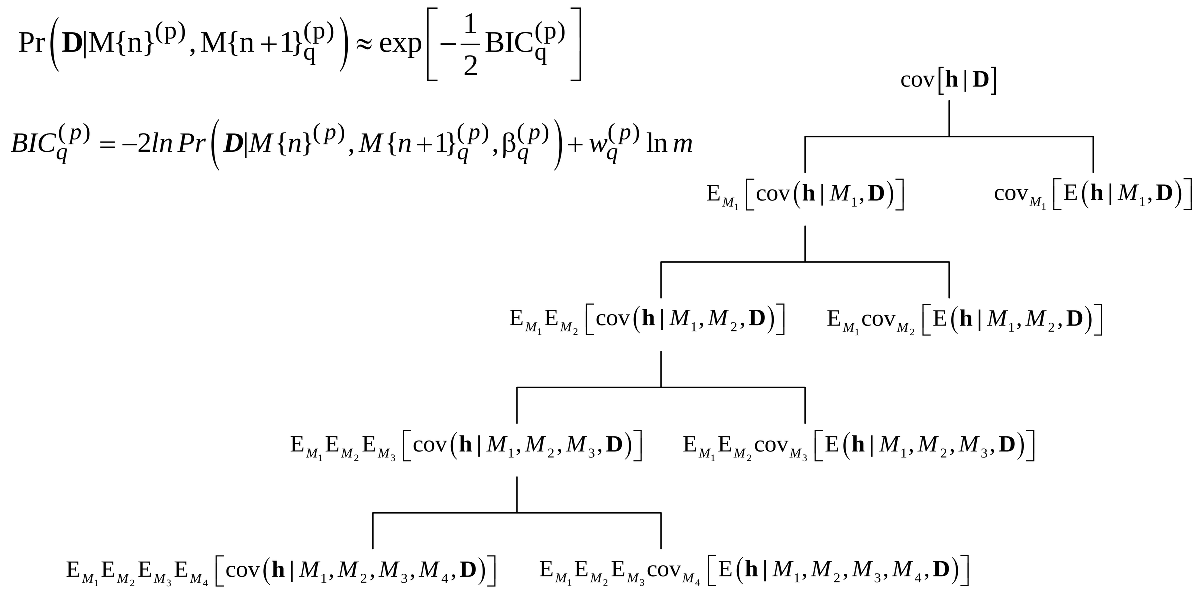

Figure(4) BMA tree for uncertainty propagation

[6] Calibration Data Uncertainty

We use 215 driller logs for model calibration. Table(1) shows two competing calibration propositions, in which we interpret the undetermined materials (i.e. driller log terms) as part of:

1) Clay assemblage complex facies
2) Sand assemblage complex facies

Table(1) Two calibration data sets

Sand	Undetermined	Clay
Data Set I Sand Facies	Data Set I Clay Facies	
(1) Sand: fine, fine packed, very fine, good, medium, coarse, loose, yellow, hard packed, packed, pay, dirty , sandstone, gray, lightly gray, tight , with shell fragments, with wood, gray-white, blue-gray (2) Sand and gravel (3) Gravel and hard sand (4) Pea gravel /with shell	(1) Sand and clay, clay and sand (2) Sand and shale, shale and sand, streaks of sand and shale (3) Shalely sand, sand and shale streaks, poor sand and streaks of shale, sand and hard sandy shale, shale with mixed gravel (4) Sand and limestone (5) Gumbo and sand (6) Gumbo, shale and sand	(1) Clay: blue, hard, soft, gray-green, brown, dark brown highly organic , tan, red-brown, green (2) Clay with sand strings (3) Shale: heavy, sandy, hard, red, brown , sandy, sticky, yellow (4) Shale with some sand breaks, shale with streaks of sand, shale and Gumbo, streaks of shale and gumbo (5) Other: gumbo , tough, rock, limestone, broken rock, lime rock
Data Set II Sand Facies		Data Set II Clay Facies

[7] Modeling Assumptions Uncertainty

If geological stationarity assumption seems inappropriate, it is helpful to divide the system into subdomains that are likely to be stationary. We adopt two propositions of stationarity:

1) Global geological stationarity over the entire model domain, since ratios of sand facies as interpreted from geophysical logs are similar in the three model subdomains
2) Local geological stationarity at each model subdomain, since geological processes of fault system activities differ

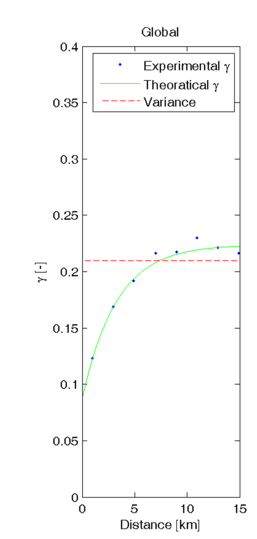

Figure(5) One global variogram describing the geological structure at each subdomain (left) differs from the local variograms describing the geological structure at each subdomain (right)

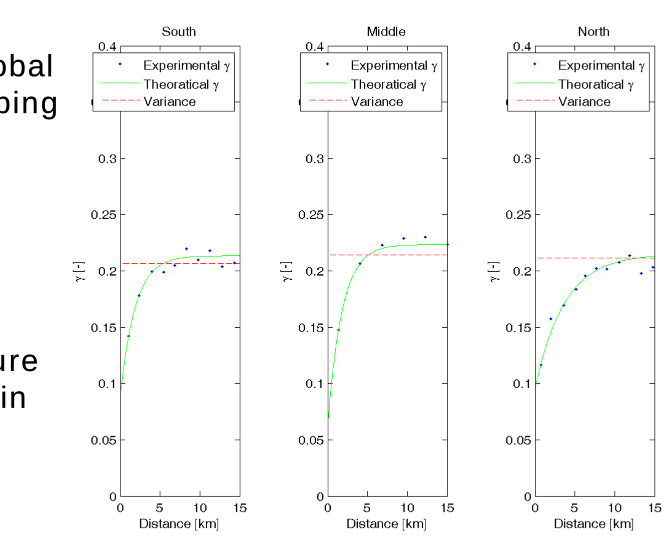

Table (2) Structural parameters for two different modeling assumptions

Variogram	Nugget	Sill	Range [km]
Global	0.087	0.137	9.8
Local south subdomain	0.0905	0.1205	6.8
Local middle subdomain	0.0705	0.1505	6.2
Local north subdomain	0.11	0.105	13.6

[8] Geological Structure Uncertainty

For mapping aquifer units with respect to fault system, while BR fault causes aquifers displacement up 105 m, Rollo [1969] maps do not recognize the DSS fault.

We adopt two geological structure propositions:

1) DDS fault causes no displacement(two model subdomains)
2) DDS fault causes displacement (three model subdomains)

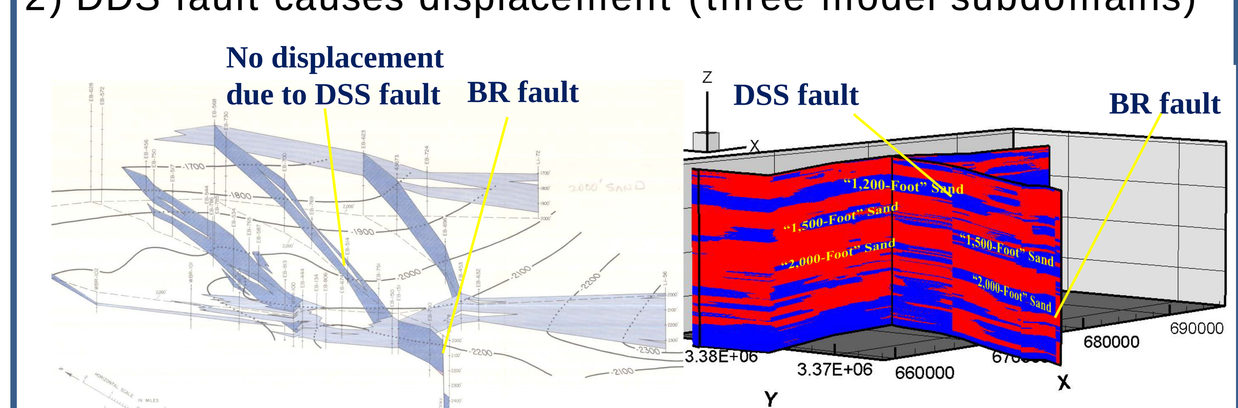

Figure(6) Rollo [1969] does not consider the DSS fault (left) resulting in 2 subdomains (i.e. south and north of the BR fault). Considering the DSS fault results in 3 subdomains (right)

[9] Mathematical Structure Uncertainty

Three competing variogram propositions:

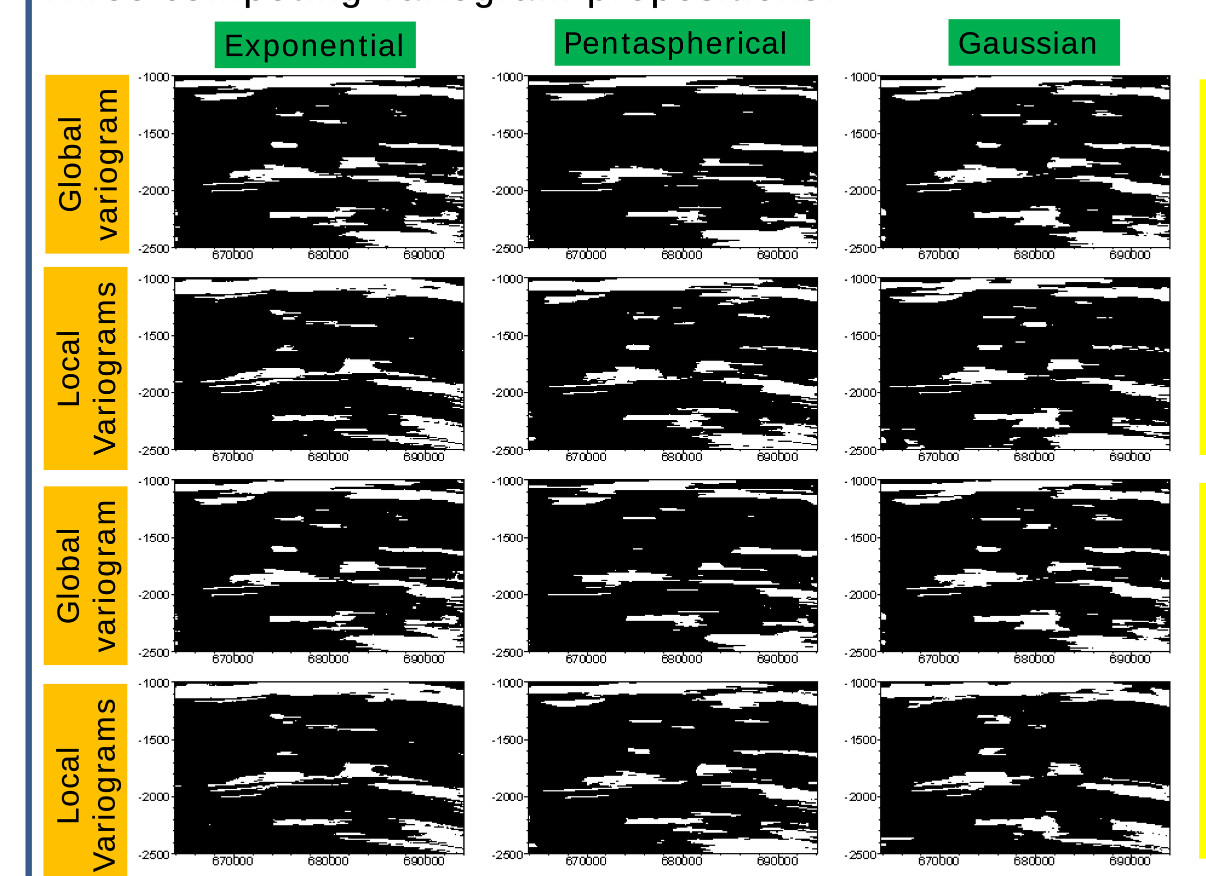

Figure(7) DSS fault diagrams for 3 mathematical models, 2 modeling assumptions and 2 calibration data sets under the geological structure proposition of three subdomains

[10] HBMA Results and Discussion

HBMA model (weighted ensemble average model)

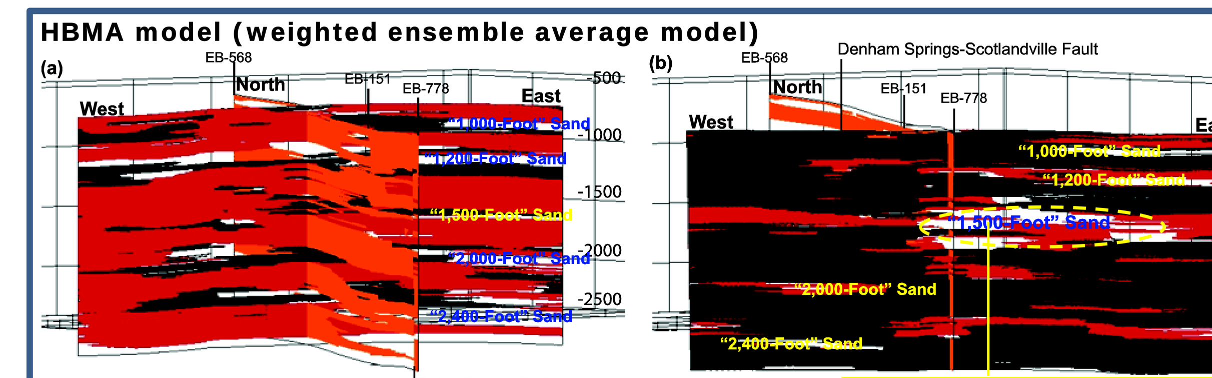

Figure(8) Leaky areas of the DSS fault illustrates good hydraulic continuity. Leaky areas of the BR fault, however, illustrates the vulnerability of the Southern Hills aquifer system.

Significant leaky areas in "1500-foot" Sand elucidates the saltwater plume [Tsai, 2010] (see Figure 1)

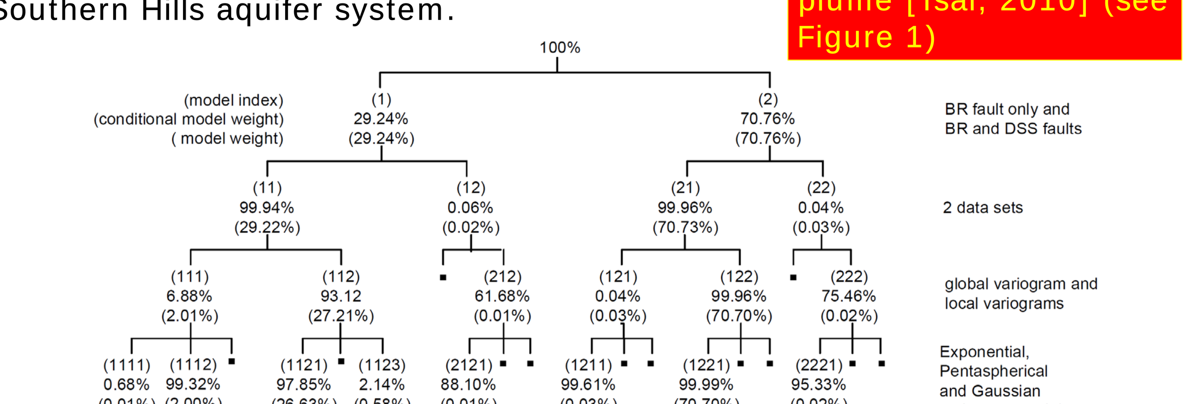

Figure (9) BMA tree for conceptual models importance (weight)

Uncertainty analysis of different modeling propositions:

1) Data: Calibration Data Set I, which is more consistent with geophysical interpretation, is significantly better
2) Geological structure: DSS fault throw is significant and should be considered in aquifer units delineation
3) Modeling assumptions: geological stationarity of aquifer subdomains with local variograms assumption is favorable
4) Mathematical structure: Exponential model is preferable in comparison to Pentaspherical and Gaussian models
5) Parameters: calibrated for each conceptual model

[11] Conclusion

- Hydrostratigraphy maps changed current geological understanding by showing that the throw of DSS fault is significant and causes aquifer units displacement
- Hydrostratigraphy maps provide insights on fault structure and leaky areas that controls the saltwater intrusion
- By testing competing propositions and using information from all models based on their model importance (model weight), we do not waste any calibration effort
- Model importance is based on the evidence of data, avoiding over-confidence in the best model that does not necessarily have a dominant model weight
- BMA tree provides an epistemic framework for evaluating sources, priorities and propagation of uncertainty.